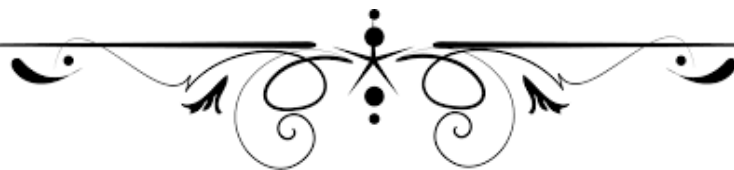


## **Chapter-6**

# *HYDROLOGICAL EVENTS EFFECTS ON CHANNEL PLANFORM*



# HYDROLOGICAL EVENTS EFFECTS ON CHANNEL PLANFORM

---

## 6.2 Introduction

Flood is a natural hydrological condition which is seasonal and often disastrous events around the Globe. It is not a localised phenomenon but occurs almost any part of the world due to heavy rainfall or release of heavy discharge in the river channel [220]. The flooded rivers represent a dynamic fluvial landscape in the world. Due to the growing population in these plains water demand increases for agricultural, domestic and industrial, which creates higher pressure on the fluvial system [221]. Such fluvial systems are the most threatened ecosystem around the Globe, where urbanisation, population, bio-invasion or changes in water regime result as degraded landscapes [203, 204].

The role of flood events in fluvial morphology is still controversial and much more debate has taken place since Wolman and Miller (1960) stated that channel planform was mainly adjusted to the frequent flood events [48, 205]. The fluvial system may be adjusted to major floods events with two years recurrent interval which control the river morphology, while moderate flood events with recurrent interval 14-30 times in a year adjust the overall morphology formed by major flood events [224]. However, the role of such extreme flood events needs to be studied to control the channel planform dynamics [225].

The morphology of river reaches and segments (e.g. stretches with a length of 101–103 m bank full channel widths) are determined by interactions between inputs of

water sediment and organic materials, and the characteristics of their boundaries including geology, land use and anthropogenic elements[208–211]. These river reach morphologies are known as hydro-geomorphological forms.Changes in river morphology due to floods results in modification of other morphological and ecological conditions until the river adapts the new environmental conditions. Rivers adjust their morphologies in response to changes in their flow regime, sediment supply, and size of the supplied sediment. However, river morphology is determined by the surrounding vegetation and the width of the alluvial valley. Morphological evolution in the large alluvial rivers is controlled by the direct human intervention (e.g. water abstraction, regulation, dams, bridges, sand mining, and river protection activities) as well as natural impact (e.g. land-use change, climate change, and population growth) which are essentialfor modelling of channel planform dynamics[212, 213]. These changes in river input parameters need to be considered for regional planning, infrastructural planning and study of erosion and sedimentation process[41, 215].

Many studies have been carried out to understand the relationship between hydrology and fluvial geomorphology, while more attention has been given to focus on the impact of discrete large flood events on river morphology [212,215–219].Very limited studies until now, have investigated the food frequency on the river morphology[235]. Phillips (2002) indicated that flash floods in a forested headwater basin, with recurrence interval>200 years, were the only floods to cause the significant channel change in ~20 years [238]. On the other hand, Dean and Schmidt (2013) found that a flood in the Rio Grande river with a recurrence interval of 13-15-years had significant effects on channel widening up to 52% [239]. Dépret et al. (2015) considered the hydrological control on the morphogenesis of low-energy meanders in

the Cher river, France [235]. They examined the duration, frequency, and intensity of floods on the changes in the river morphology and demonstrated that the river morphology was controlled by low magnitude hydrological events. However, Hooke (2016b) investigated morphological impacts of the flood of varying magnitude in a semiarid region and found, the opposite results as the river flows without significantly changing fluvial morphology [234]. Therefore, it is essential to assess the effects of hydrology on river evolution; especially the effects of extreme hydrological events on river morphology in the highly dynamics river like Ramganga.

Alluvial rivers are very sensitive to the flow condition and can readjust planform produced by water and sediment input, active tectonics, and anthropogenic activities occur at various temporal and spatial scale. Any changes in natural or anthropogenic activities can initiate a shift from a state of dynamic equilibrium. This results in the channel instability causing changes in channel planform and pattern. In order to understand the channel planform dynamics, a multidisciplinary approach is required. Large tropical rivers, especially Himalayan rivers, show very high discharge and sediment load during the monsoon season which results in the high channel migration rate and extensive riverbank erosion in the flood plain. In the last few decades, Geoinformatics based tools and techniques play an essential role in the study of fluvial geomorphic processes at the global scale.

The term catastrophic event in the fluvial processes indicates an extremely rare occurrence of high discharge that produces major modification in channel morphology. Such a catastrophic flood event requires (a) infrequency, and (b) a high magnitude to exceed the threshold value which bounds the normal equilibrium state of a particular fluvial system [240]. Hydrologist has developed standard methods for flood frequency

analysis, but these methods don't explain the impact of the flood on river morphology[241].

Moreover, India is one of the most flood-prone countries in the world except Bangladesh, and about 40 million hectares of land, roughly one-eighth of the country's geographical area, is prone to floods [242]. High-magnitude floods in Indian rivers are responsible for fluvial erosion and sediment transport. For most of the large rivers, the ratio between mean annual flood and rare, extreme floods is high, which is 1.3 to 4.0 [243]. This ratio is also higher for smaller rivers. The monsoon-dominated rivers, with high variability in discharge, have the ability to alter floodplain and channel morphology in a significant way [167, 226]. Flood is an annual phenomenon that occurs in most of the Himalayan rivers. These flood events have a small impact on channel morphology, and some others have a more massive impact which persists for a longer time in the morphology. There are many other examples of catastrophic floods that have modified the river planform in significant ways. The impact of the large flood on channel morphology has been summarized by Gupta (1988) which are (i) increase in incompetence, (ii) widening of channel, (iii) deposition of a large amount of coarse gravel within the channel, (iv) scouring of flood plains, (v) formation of channel-in-channel physiography and (vi) the erosion of bars[185].

This main objective of this chapter is to assess the role of flood frequency on the morphological evolution of the Ramganga river. The relationship between flood events and fluvial morphological indices could be beneficial for better management of fluvial systems.

Figure 6.1 shows the location of different meander loops in segment A and segment B. The figure also shows the location of the hydrological station from where the hydrological data is collected for the analysis.

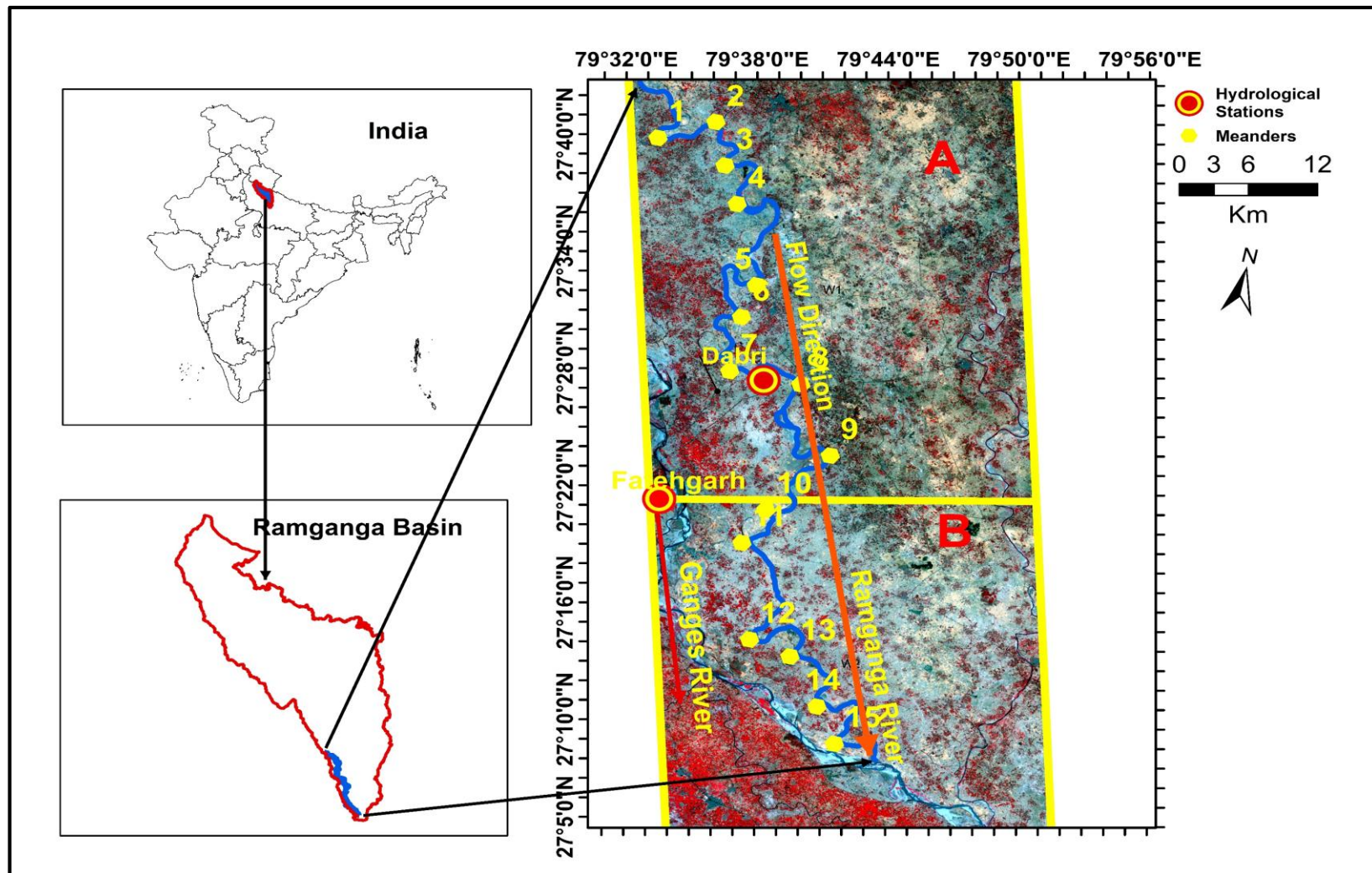


Figure 6.1 Location of different mender loops in segment A and segment B

### 6.3 Data used

Landsat images and topographic maps were used to analyse changes in the river morphology along with the hydrological data (Table 6.1). The hydrological data, including average daily discharge and yearly maximum discharge at the Dabri hydrological station, were analysed for a long period (1985-2019) as mentioned in *Appendices A*. The Dabri station is the nearest hydrological station to the study reach, located about 40 km upstream of the confluence point of Ganga and Ramganga river (Fig. 6.1). No significant tributaries join the Ramganga river between the gauging station and the confluence point. Therefore a significant change in flow regime along the study reach is not possible.

*Table 6.1 List of spatial data and hydrological data sources*

<b>Data</b>	<b>Spatial Resolution</b>	<b>Date</b>	<b>Provider</b>	<b>Use</b>	<b>Discharge (m<sup>3</sup>/s)</b>
Landsat MSS	80 m	1973	USGS	Channel analysis	-
Landsat MSS	80 m	1981	USGS	Channel analysis	-
Landsat MSS	80 m	1985	USGS	Channel analysis	246.25
Landsat TM	30 m	1990	USGS	Channel analysis	213.19
Landsat TM	30 m	1995	USGS	Channel analysis	104.84
Landsat ETM+	30 m	2000	USGS	Channel analysis	240.01
Landsat ETM+	30 m	2005	USGS	Channel analysis	222.38
Landsat TM	30 m	2010	USGS	Channel analysis	320.66
Landsat TM	30 m	2015	USGS	Channel analysis	101.21
Landsat OLI	30 m	2019	USGS	Channel analysis	191.74
Topographic sheets	1:50,000	2006	Survey of India	Channel analysis / Geometric correction	-
Hydrological data	Dabri hydrological Station	1985-2019	CWC	Hydrological analysis	-

## 6.4 Methodology

The topographic map of 2006 is considered as a base map for the georeferencing of the remote sensing images. Geometric corrections were applied on the topographic map according to 60 ground control points in the stable area along the river. Geometric correction of these images was done with a second-order polynomial transformation method in the ArcGIS 10.1 software. The total errors were estimated using root mean standard error (RMSE), and which is less than 1 pixel. Using true composite images in Landsat data (Red, Green, and Blue bands), the river planform is digitised in Arc GIS [227, 228].

Based on 2019 Landsat OLI image, the study reach was divided into 15 meander loops. Using Fluvial Corridor 10.1, the active channel width ( $w$ ) was determined in 10 m intervals, and changes were detected along the entire ~ 125 km reach of the Ramganga river. In addition, the sinuosity index (Eq. 6.1), straight meander length ( $L$ ), centerline flow length ( $S$ ), erosion area ( $EA$ ), erodible length ( $EL$ ), channel migration ( $M$ ), (Eq. 6.2), and radius of curvature ( $R_c$ ), were calculated to provide morphological indices [229–231].

$$P = \frac{L_{cmax}}{L_R} \quad (6.1)$$

Where  $P$  is sinuosity index,  $L_{c\ max}$  is the length of the midline of the channel (in the single-channel), and  $L_R$  is the overall length of the reach.

The migration of the centerline was measured with the help of ‘migration polygons’ which were drawn on adjacent and sequential centerlines (Fig.2.3). The respective total area of a migration polygon was then divided by half of the perimeter of that polygon or the length of the migration polygon centerline. The migration rates



of channel centerlines were then measured by using the following formula, as suggested by Giardino and Lee (2011)[249].

$$Rm = (A/L)/Y \quad (6.2)$$

Where,  $R_m$  is the migration rate;  $A$  is the polygon area,  $L$  is the length of centerline for each polygon, and  $y$  is the time interval involved in the computation.

To identify meander evolution, there are various classes and models available, and most of these methods are derived from different case studies[81, 233]. In the present study, meander loop changes and their evolution have been defined using's Hooke (1984) model, as shown in Figure 6.8[85]. This model also has been used by Yousefi et al. (2016) for detecting the morphological changes in the Karoon river in Iran[53].

For the Dabri gauge station using the maximum yearly discharge data, the flood recurrence interval was calculated for 2, 5, 10, 25, 50, and 100-years, by Log-Pearson type III distribution. In addition, using average daily discharge, the frequency (number of flood days per year) of the different recurrence interval discharges was calculated for all discrete study periods (Tables 6.6).

Here, Pearson correlation test was used to analyse the relationship between the frequency of the different recurrence interval discharge and change in morphological indices in the Dabri Station[235]. Figure6.2 shows a flowchart of the methodology used in the present study.

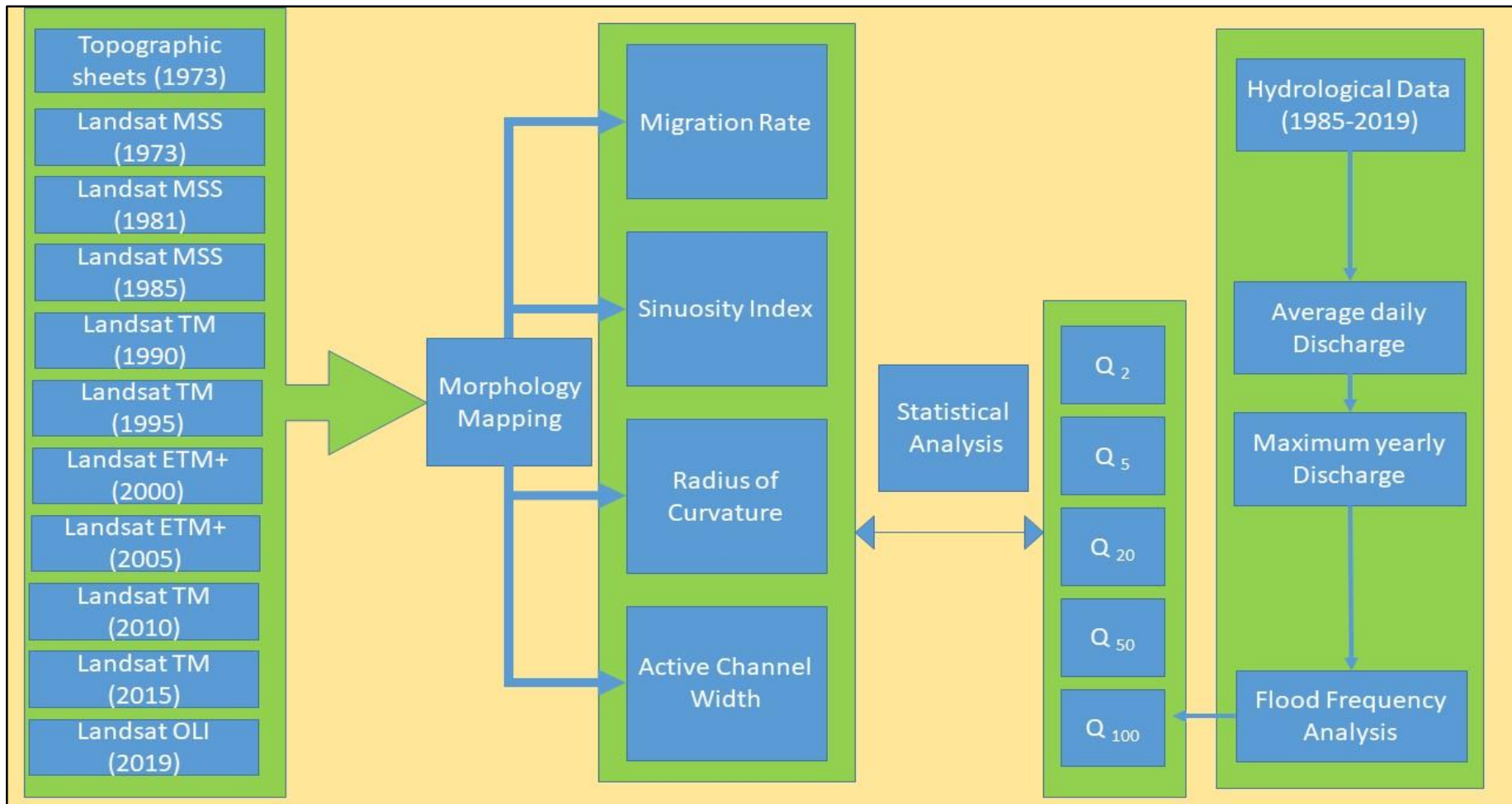


Figure 6.2 Methodology used in the study

## 6.5 Results geomorphological evolution

### 6.1.1 Width of the active channel

The average width of the active channel along the study reach (~ 125 km) narrowed down significantly by ~43% between 1973 and 2019 (Fig.6.3). In section A, the active channel width reduced from 1973 to 2000 and after that, it started to increase to the present condition due to an increase in the water discharge in the channel (Fig.6.3 A). The channel width decreased from 1973 to 2000 period is about 110 m. In section B, the average width is observed less than the upstream channel (Fig.6.3 A). This reduction in the active channel width is observed due to controlled water discharge from the dams, which is constructed in the upstream areas of the Ramganga river ([18]).

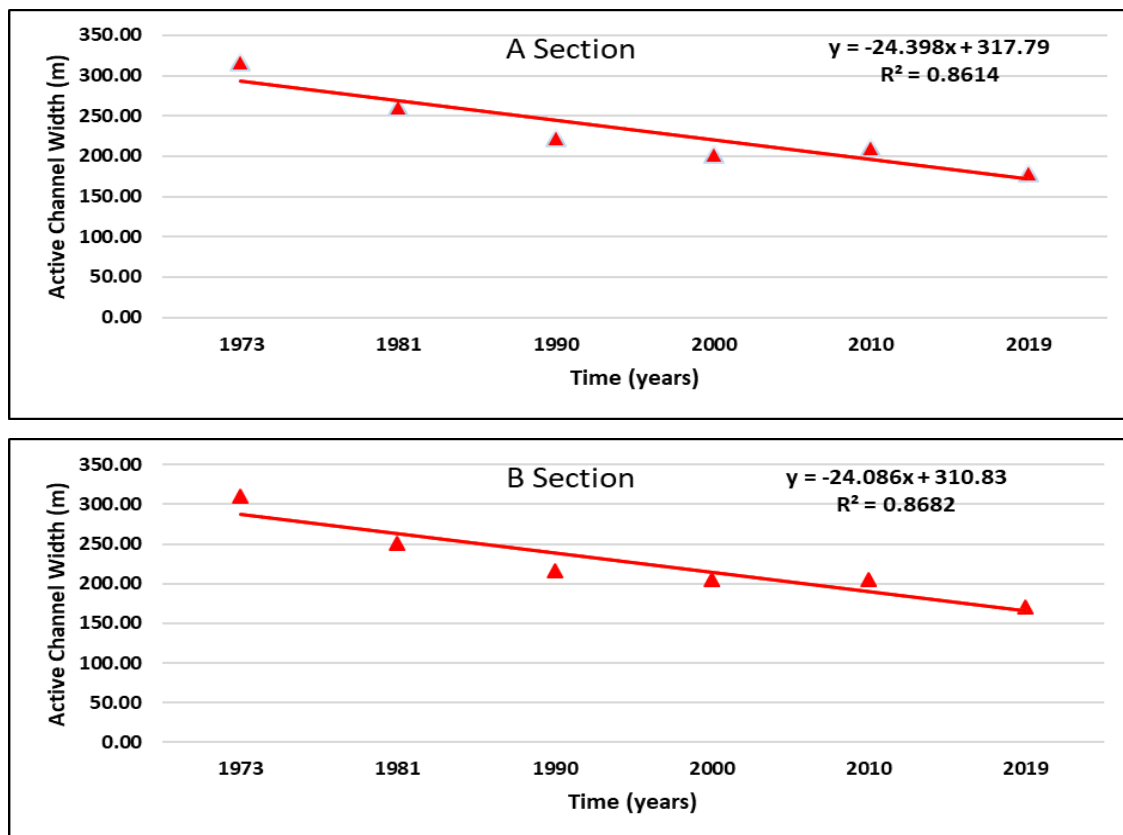


Figure 6.3 Active channel width evolution and its trend

### 6.1.2 Radius of curvature

The radius of curvature ( $R_c$ ) measures of the ‘tightness’ of a single meander bend and is inversely correlated with sinuosity. The  $R_c$  is measured by the radius of a circle that fits the meander arc from the outside of the bank-full channel to the crossing point of two lines that perpendicularly bisect the tangent lines of each meander departure point (Fig.6.5).

Meander no. 12, which is near to the Baran village is very dynamic in nature due to erosional possess of the river. Trends in  $R_c$  of this meander in the study reach appears like unidirectional reducing (Fig. 6.4). The reduction in  $R_c$  initially started from 1973 to 2019. The overall reduction in the radius of curvature is 450m detected in this meander from 1973 to 2019. This shows the potential site of the meander neck cut off in the future, which will eventually reduce the valley length of the river. This neck cut off will change the morphology in the downstream area.

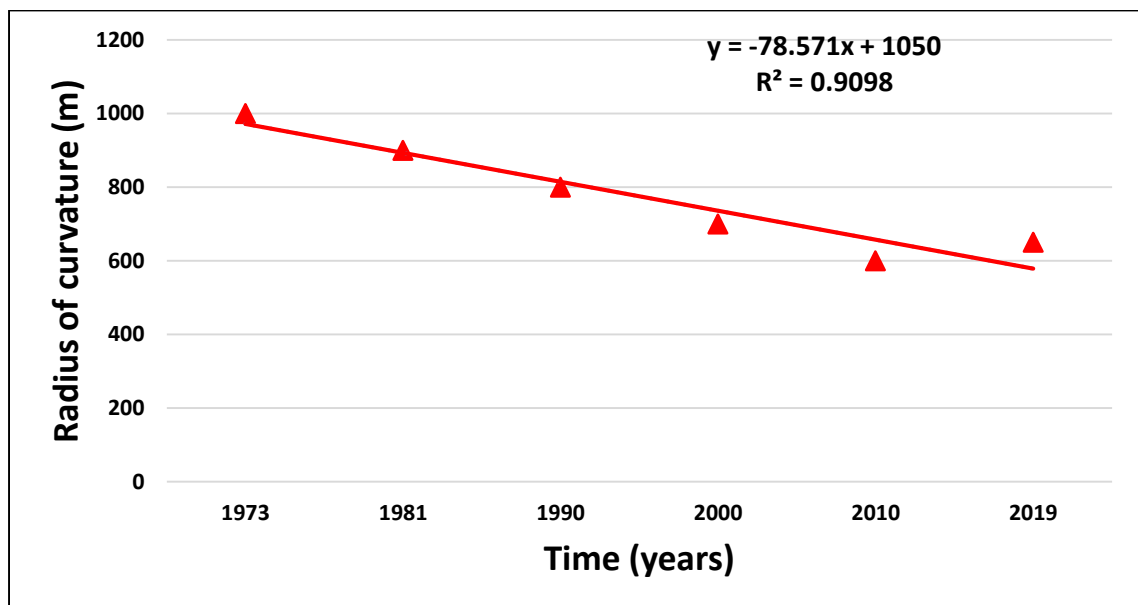


Figure 6.4 Evolution of curvature radius during 1973-2019

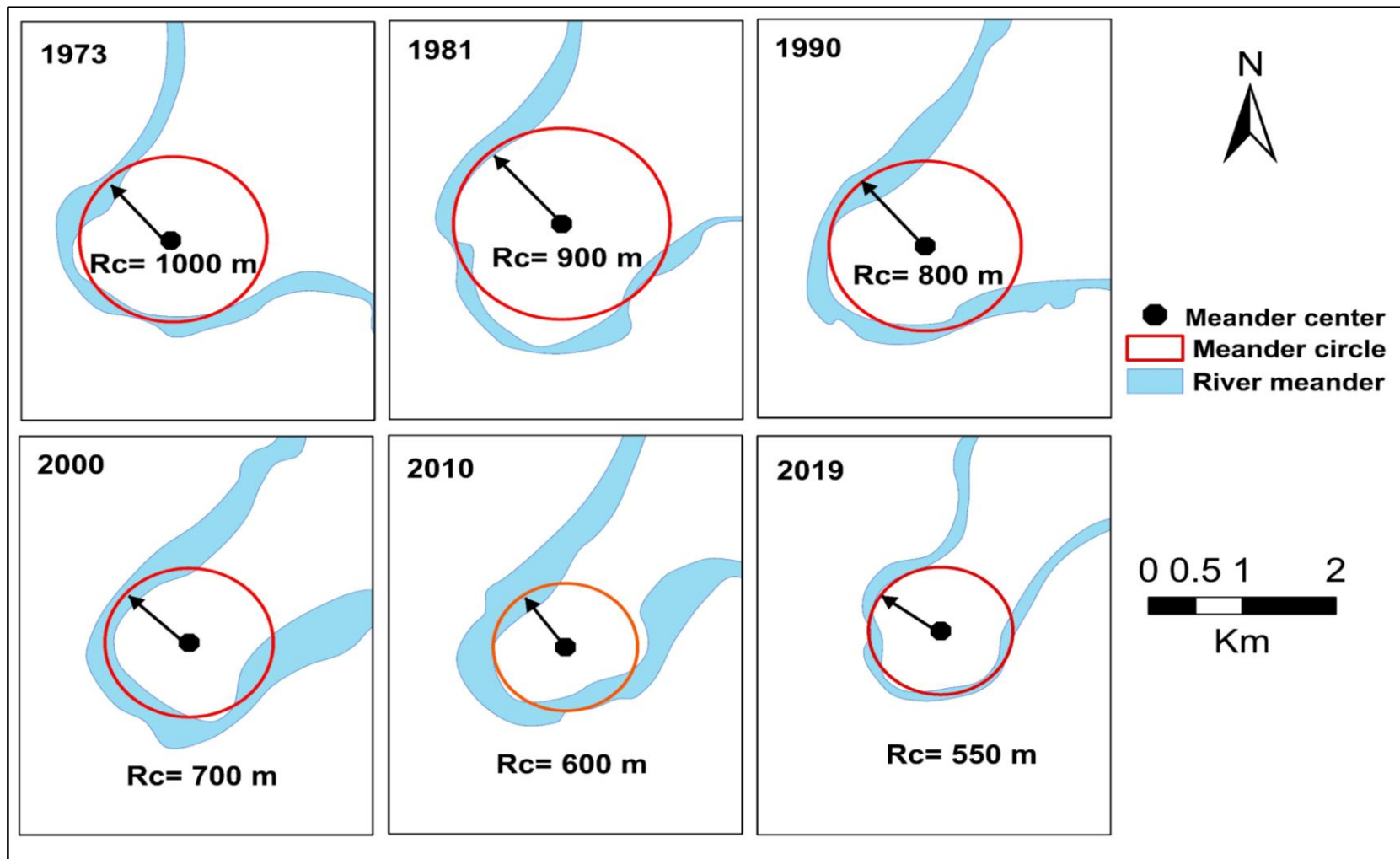


Figure 6.5 Temporal measurement of radius of curvature of meander 12.

### 6.1.3 Sinuosity index

The entire study area is highly sinuous in nature which shows the index value more than 1.5 (Figure 6.6). The general trend of sinuosity index shows that sinuosity of the channel reduced in last five decades (1973-2010) while a dramatic increase in the index is found in the entire study reach in 2019. This gives a clue about the morphological characteristics of the river that the river is highly meandering in nature. Results showed that in section A, the average sinuosity index decreases from 1.87 to 1.69, suggesting an overall straightening of the river course during 1973 to 2010 (Fig. 6.6 A). In Section B, the same trend is observed with a slightly higher value of sinuosity index. From 1973-2019 a reduction of 1.88 to 1.71. The sinuosity value was notably higher in 1973 (1.88) and the lowest in 2010 (1.71). A dramatic increase in the index is also observed in both section in the year 2019 (Fig. 6.6 B).

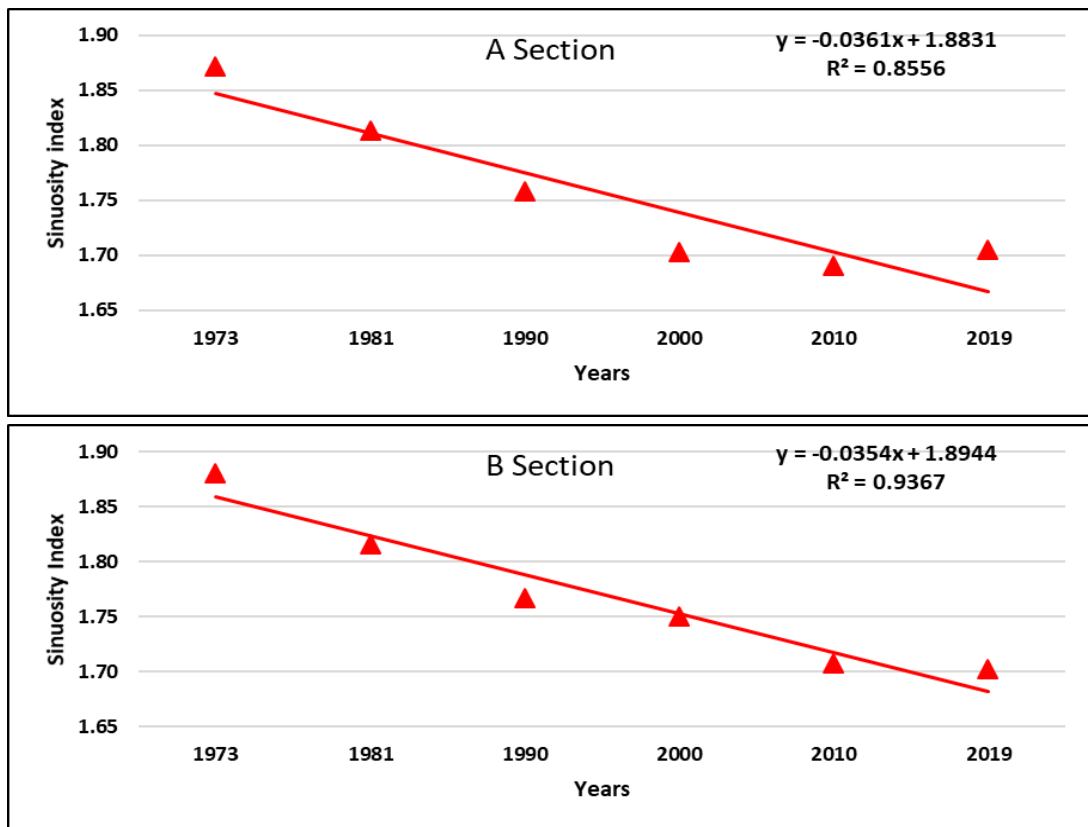


Figure 6.6 Evolution of sinuosity index in study reach

### 6.1.4 Channel migration

Channel migration rate in the present study is calculated for decadal-scale (Fig. 6.7). The general trend of the rate of migration is reduced in the study period 55 m/y to 22 m/y (1973-2019). The average migration rate was calculated ~33 m/y. In section A the highest migration rate is observed in the ~50 m/y during (1973-1981) and the lowest ~22 m/y in the (2010-2019) (Fig. 6.7 A). In section B, the same trend of migration rate was also observed with the highest migration rate ~ 55 m/y (1973-81) and lowest ~23 m/y (2010-2019) (Fig. 6.7 B). These high migration rate is observed due to the dynamic nature of the lower reaches and low gradient of the channel. The high erosion rate in another region is also responsible, which is due to the frequent flood condition in the study area.

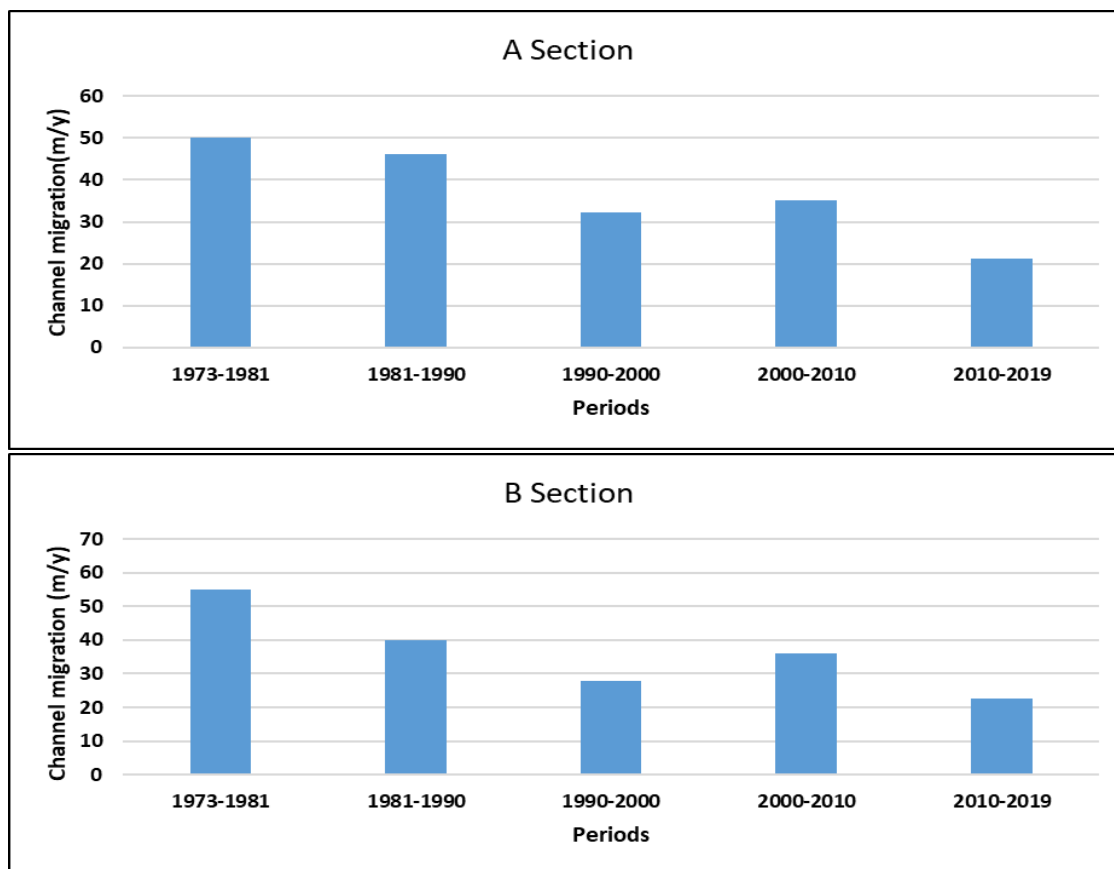


Figure 6.7 Channel migration during five periods in study area

### **6.1.5 Morphological evolutions of meander loops**

The morphological evolution of the Ramganga river is assessed from 1990 due to availability of hydrological data and to find out the correlation with channel migration rate. The changes in the meander loop and their evolution were classified on the basis of Hooke's (1984) change model (Fig.6.8). Results show that most of the meander loops extended and expanded with a triple combination (Table 6.2 and 6.3). In the study period, all types of meander change were observed, e.g. simple, double and in triple combination during (1973-2019).

Total of eleven meander cutoff is formed during the study period. In section A, all types of meander migration are observed, and two new meander loop was formed during 1990-2000. In this phase, the mainly simple and triple combination of meander loop evolution is observed (Fig. 6.9). All type of meander evolution is observed except one in double combination (rotation and expansion). In the second phase, one new meander formed with two cutoffs during 2000-2010. In the third phase, a mainly simple type of meander evolution is observed, and one new meander with three cutoffs is observed during (2010-2019) (Table 6.2).

In the downstream section B, the same phenomena are observed with high meander dynamics in the floodplain. In this section, a mainly simple and double combination of meander evolution is observed (Fig.6.10). In the first phase of study extension of the meander, the loop is observed mainly in four meanders, and two cutoffs with one new meander loop are evolved during 1990-2000. In second meander lateral movement is also observed. In the second evolution period, mainly simple and double combination type of evolution is observed with one cutoff during 2000-2010. In this period no new meander is evolved. In the last phase, a mainly simple type of evolution is observed. In this phase, also, no new cutoff is formed, and one new meander is developed during (2010-2019) (Table 6.3). In meander 12, which is a continuous extension is observed in two phases, and in the last phase, it started to decrease in its previous position.



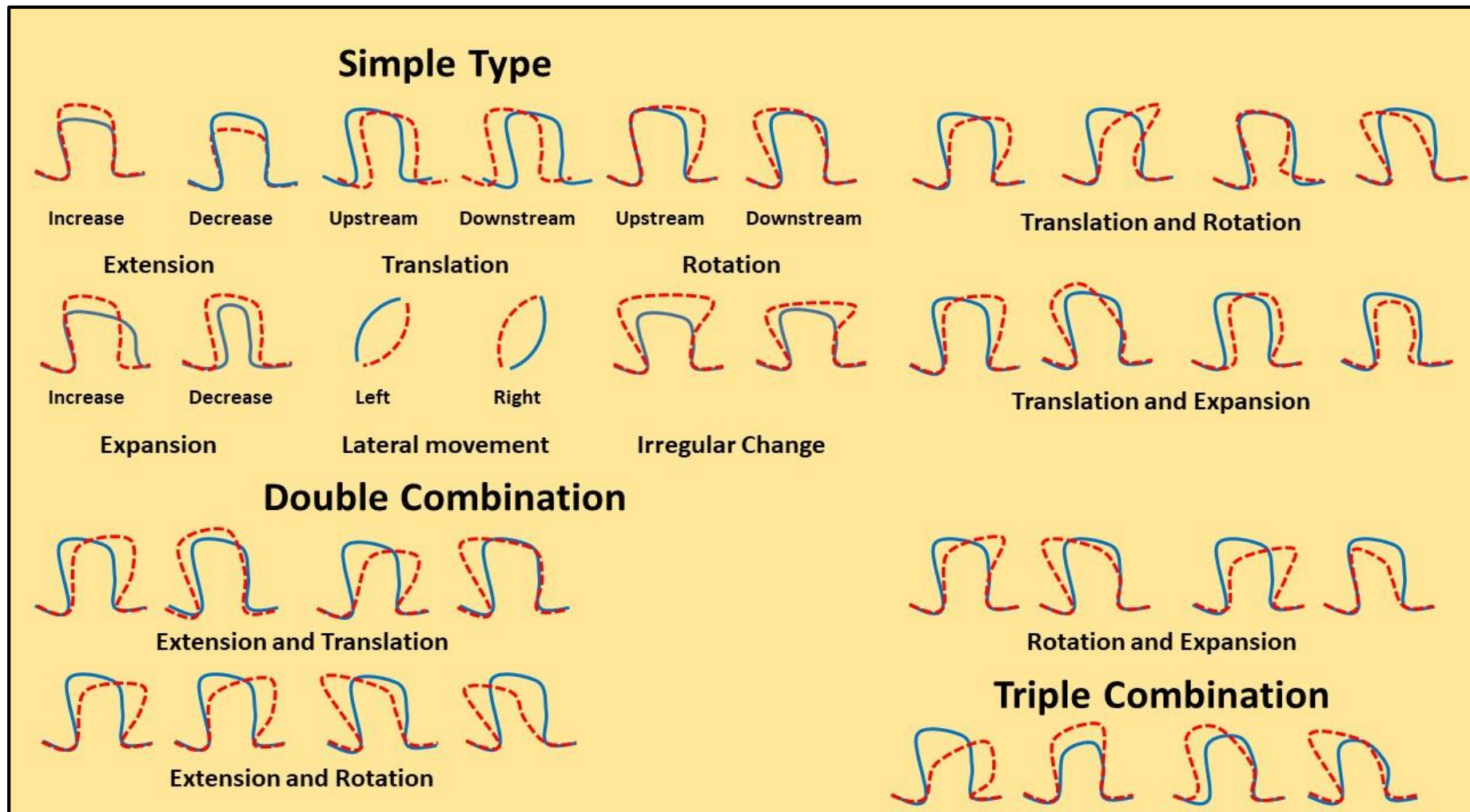


Figure 6.8 Model of meander change based on Hooke (1984)

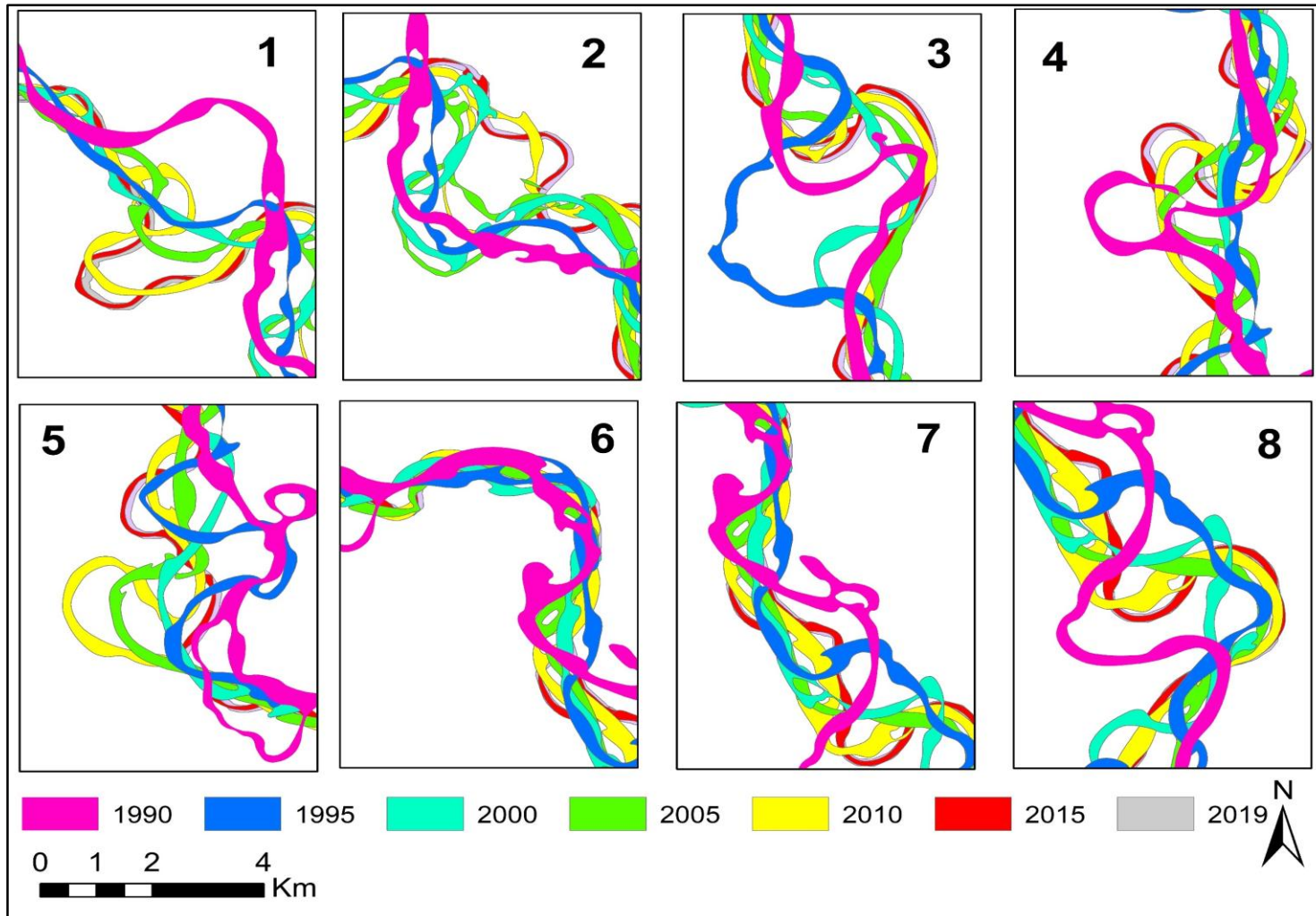


Figure 6.9 Morphological evolutions in some meander loops in the Ramganga River

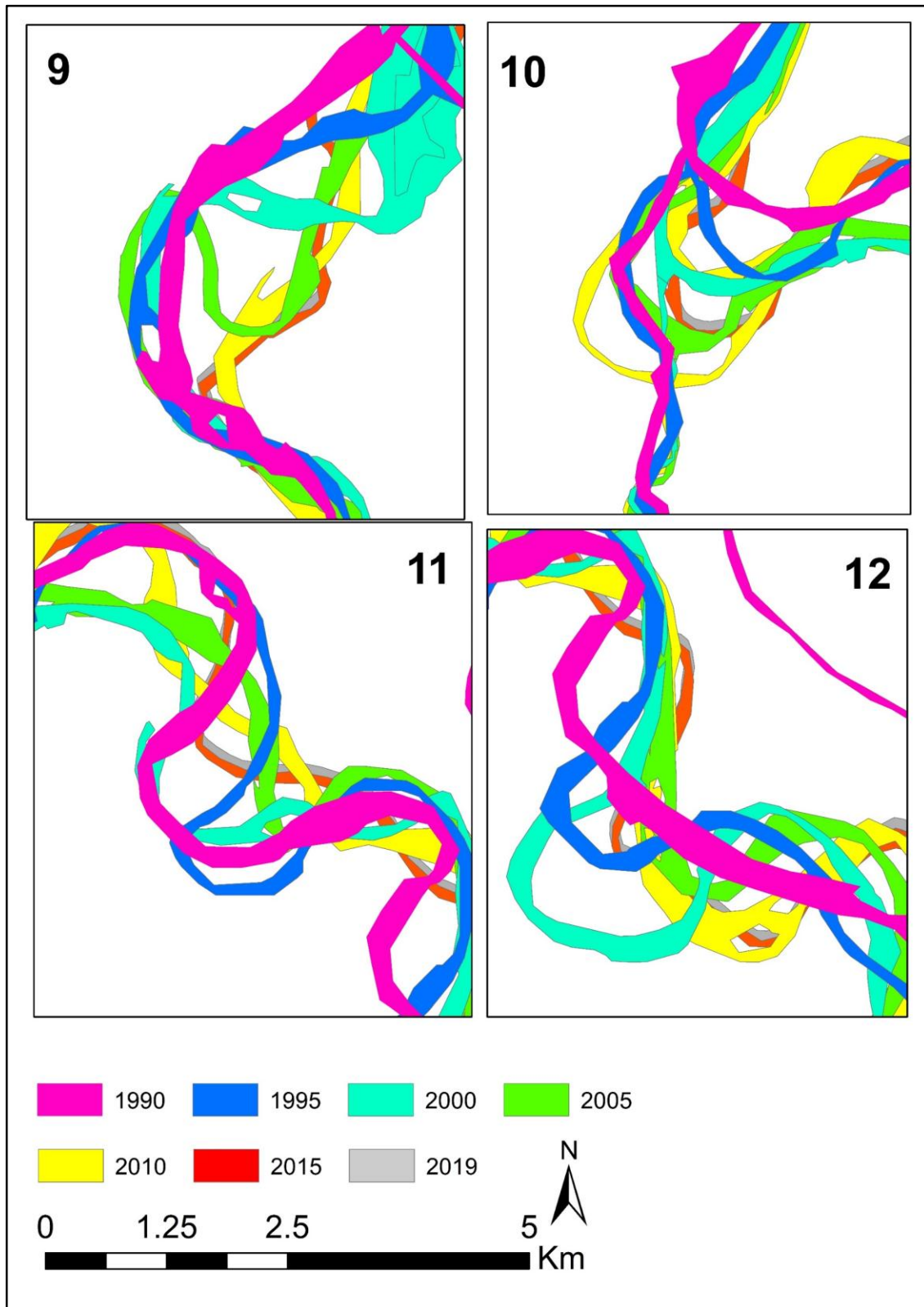


Figure 6.10 Morphological evolutions in some meander loops in the Ramganga River

*Table 6.2 Frequency of meanders change in a different type of evolution In Segment A*

<b>Frequency of meanders change in a different type of evolution A</b>									
<b>Change</b>	<b>Simple types</b>			<b>Double combinations</b>			<b>Triple combinations</b>		
<b>Period</b>	<b>Extension</b>	<b>Translation</b>	<b>Lateral movement</b>	<b>Extension and Expansion</b>	<b>Translation and Rotation</b>	<b>Rotation and Expansion</b>	<b>Extension, Translation and Rotation</b>	<b>New meander</b>	<b>Cut off</b>
1990-2000	4	3	2	2	1	0	1	2	2
2000-2010	3	2	1	1	1	1	0	1	2
2010-2019	4	3	1	2	0	0	0	1	3

*Table 6.3 Frequency of meanders change in a different type of evolution In Segment B*

<b>Frequency of meanders change in a different type of evolution B</b>									
<b>Change</b>	<b>Simple types</b>			<b>Double combinations</b>			<b>Triple combinations</b>		
<b>Period</b>	<b>Extension</b>	<b>Translation</b>	<b>Lateral movement</b>	<b>Extension and Expansion</b>	<b>Translation and Rotation</b>	<b>Rotation and Expansion</b>	<b>Extension, Translation and Rotation</b>	<b>New meander</b>	<b>Cut off</b>
1990-2000	4	1	2	1	1	1	1	1	2
2000-2010	4	2	1	1	1	1	0	0	1
2010-2019	2	1	1	1	0	1	0	1	1

## **6.6 Flood Frequency Analysis**

Flood Frequency Analysis (FFA) is a statistical measure that is most commonly being carried out for predicting and quantifying the discharge of floods at a particular location of a river on desired time intervals. The occurrence probabilities of various flood sizes can be determined through probability distribution techniques of varied types that generally include normal, and log-normal, distributions;

In the present study thirty-four years (1986-2019) of annual maximum peak discharge data were used for analysis (Fig. 6.11). The size of the sample data can be considered reliable for projecting discharge scenarios. The data has been collected for the Dabri gauge station from CWC. In order to perform the flood frequency analysis of river Ramganga river, Log-Pearson Type III Distribution have been used to predict the probable floods of different recurrent intervals as described below.

### **6.1.6 Log-Pearson Type III (LP3)**

The Log-Pearson Type III distribution is a statistical technique for fitting frequency distribution data to predict the design flood for a river at some site. Once the statistical information is calculated for the river site, a frequency distribution can be constructed. The probabilities of floods of various sizes can be extracted from the curve. The advantage of this particular technique is that extrapolation can be made of the values for events with return periods well beyond the observed flood events. This technique is the standard technique used by Federal Agencies in the United States. The Log-Pearson Type III distribution tells us the likely values of discharges to expect in the river at various recurrence intervals based on the available historical record. This is helpful while designing structures in or near the river that may be affected by floods. It is also helpful when designing structures to protect against the largest expected event.

In log-Pearson type-III (Pearson, 1916) probability distribution, the variate is first transformed into logarithmic form (base 10), and the transformed data is analysed for the random hydrological series[251].

Then the series of Z variates, where  $Z = \log x$  are first obtained.

For this Z series, for any recurrence interval T from the equation

$$\chi_T = \bar{\chi} + K\sigma \quad (6.3)$$

$$Z_T = \bar{Z} + K_Z\sigma_Z \quad (6.4)$$

Where,  $K_Z$  is the frequency factor which is a function of recurrence interval (T), and  $C_S$  the coefficient of skewness.

$\sigma_Z$  is the standard deviation of the variate sample

$$\sigma_Z = \sqrt{\Sigma(Z - \bar{Z})^2 / (N - 1)} \quad (6.5)$$

$C_S$  the coefficient of skewness.

$$C_S = \frac{N \Sigma(Z - \bar{Z})^3}{(N - 1)(N - 2)(\sigma_Z)^3} \quad (6.6)$$

Where,  $\bar{Z}$  is the mean of z value and N is the sample size, i.e., number of recorded years; after obtaining the values of  $Z_T$ , the analogous values of  $\chi_T$  is attained by the equation  $Z = \log x$ , as  $\chi_T = \text{antilog } Z_T$ .

The Log-Pearson Type III distribution analysis was done following the above methodology, and the results obtained are shown in Table 6.4 and Table 6.5.

*Table 6.4 Computation of statistical parameters for Dabri gauge station*

Rank	Year	Q Peak (m <sup>3</sup> /s)	Y=log Q	$(Y - \bar{Y})^2$	$(Y - \bar{Y})^3$	Return Period $T = \frac{n + 1}{m}$	Exedence Probability $P = \frac{1}{T}$
1	2001	7468.74	3.873	0.3300	0.1896	35.00	0.03
2	1986	6225.52	3.794	0.2454	0.1216	17.50	0.06
3	1999	5891.78	3.770	0.2223	0.1048	11.67	0.09
4	1994	5500.00	3.740	0.1950	0.0861	8.75	0.11
5	1989	5180.00	3.714	0.1727	0.0718	7.00	0.14
6	2000	4841.02	3.685	0.1491	0.0576	5.83	0.17
7	2006	4660.84	3.668	0.1367	0.0505	5.00	0.20
8	2012	4650.78	3.668	0.1360	0.0501	4.38	0.23
9	2011	4570.62	3.660	0.1305	0.0471	3.89	0.26
10	1996	3875.26	3.588	0.0838	0.0243	3.50	0.29
11	2004	3573.90	3.553	0.0647	0.0165	3.18	0.31
12	2002	3156.99	3.499	0.0402	0.0081	2.92	0.34
13	2009	2736.34	3.437	0.0192	0.0027	2.69	0.37
14	1987	2572.57	3.410	0.0125	0.0014	2.50	0.40
15	1991	2410.06	3.382	0.0069	0.0006	2.33	0.43
16	2005	2204.37	3.343	0.0020	0.0001	2.19	0.46
17	1997	1924.31	3.284	0.0002	0.0000	2.06	0.49
18	1995	1846.00	3.266	0.0011	0.0000	1.94	0.51
19	1990	1662.26	3.221	0.0061	-0.0005	1.84	0.54
20	2003	1369.72	3.137	0.0263	-0.0043	1.75	0.57
21	2010	1308.10	3.117	0.0332	-0.0060	1.67	0.60
22	2007	1230.11	3.090	0.0436	-0.0091	1.59	0.63

23	1998	1195.75	3.078	0.0489	-0.0108	1.52	0.66
24	2008	1096.39	3.040	0.0670	-0.0173	1.46	0.69
25	1992	1000.89	3.000	0.0890	-0.0266	1.40	0.71
26	2016	994.87	2.998	0.0906	-0.0273	1.35	0.74
27	2019	991.92	2.996	0.0914	-0.0276	1.30	0.77
28	2015	971.09	2.987	0.0970	-0.0302	1.25	0.80
29	2014	914.11	2.961	0.1141	-0.0385	1.21	0.83
30	2017	790.32	2.898	0.1608	-0.0645	1.17	0.86
31	1993	760.25	2.881	0.1746	-0.0729	1.13	0.89
32	2018	728.85	2.863	0.1902	-0.0830	1.09	0.91
33	2013	712.16	2.853	0.1991	-0.0888	1.06	0.94
34	1988	503.59	2.702	0.3560	-0.2124	1.03	0.97
		2632.93	3.299	3.7361	0.1129		
		Variance	0.1132				
		Standard deviation	0.3365				
		Skew coefficient	0.0954				

**Table 6.5 Flood frequency estimates of Ramganga river using Log Pearson Type III distribution (Dabri station)**

Return Period (Tr)	K <sub>Lower</sub>	K <sub>Upper</sub>	Slope	K <sub>Calculated</sub>	$y_r = \bar{y} + k\sigma$	$Q_T = (10)^{y_r}$ (m <sup>3</sup> /s)
2	-0.148	-0.164	-0.16	-0.02	3.29	1960.08
5	0.769	0.758	-0.11	0.86	3.59	3866.21
10	1.339	1.340	0.01	1.33	3.75	5579.43
25	2.018	2.043	0.25	1.82	3.91	8129.90
50	2.498	2.542	0.44	2.14	4.02	10475.08
100	2.957	3.022	0.65	2.43	4.12	13114.43
200	3.401	3.489	0.88	2.69	4.20	16028.03



## 6.7 Hydrology and geomorphology

The average annual discharge and the annual peak discharge during the study period is given in Figure 6.11. The results of Log-Pearson type III distribution gives the 2-year ( $Q_2$ ), 5-year ( $Q_5$ ), 10-year ( $Q_{10}$ ), 25-year ( $Q_{25}$ ), 50-year ( $Q_{50}$ ), and 100-year ( $Q_{100}$ ) recurrence interval discharge in the Dabri gauging station, which are 1960, 3866, 5479, 8129, 10475 and 13114  $\text{m}^3 \text{s}^{-1}$ , respectively (Table 6.5). The frequency (number of flood days per year) of different recurrence interval discharges in study periods are given in Table 6.6. Results show that in just three periods (1990-1994, 1995-1999, 2000-2004) flood with a magnitude of more than  $Q_{10}$  has occurred in the study reach. As the number of hydrological events bigger than  $Q_{10}$  did not occur since 2005, we considered only the relationship between morphological evolution and  $Q_2$  and  $Q_5$  events (Table 6.7).

The results of a Pearson correlation test show a positive correlation between sinuosity change and radius of curvature versus frequency of events higher than  $Q_2$  at a 5% significant level. In addition, there is a significant direct correlation at the 5% level between the frequency of the events bigger than  $Q_5$  and migration (Table 6.8 and Fig. 6.14). There is a high correlation observed in the radius of curvature with the frequency of events higher than  $Q_2$  and  $Q_5$  at a 5% significant level. This statistical test also shows that there is no significant correlation between active channel width change and hydrological events of  $Q_2$  and  $Q_5$  magnitude. Which shows the other factor like human intervention (control discharge from Dam) in the channel are mainly responsible for this reduction in channel width (Table 6.8 and Fig. 6.13).

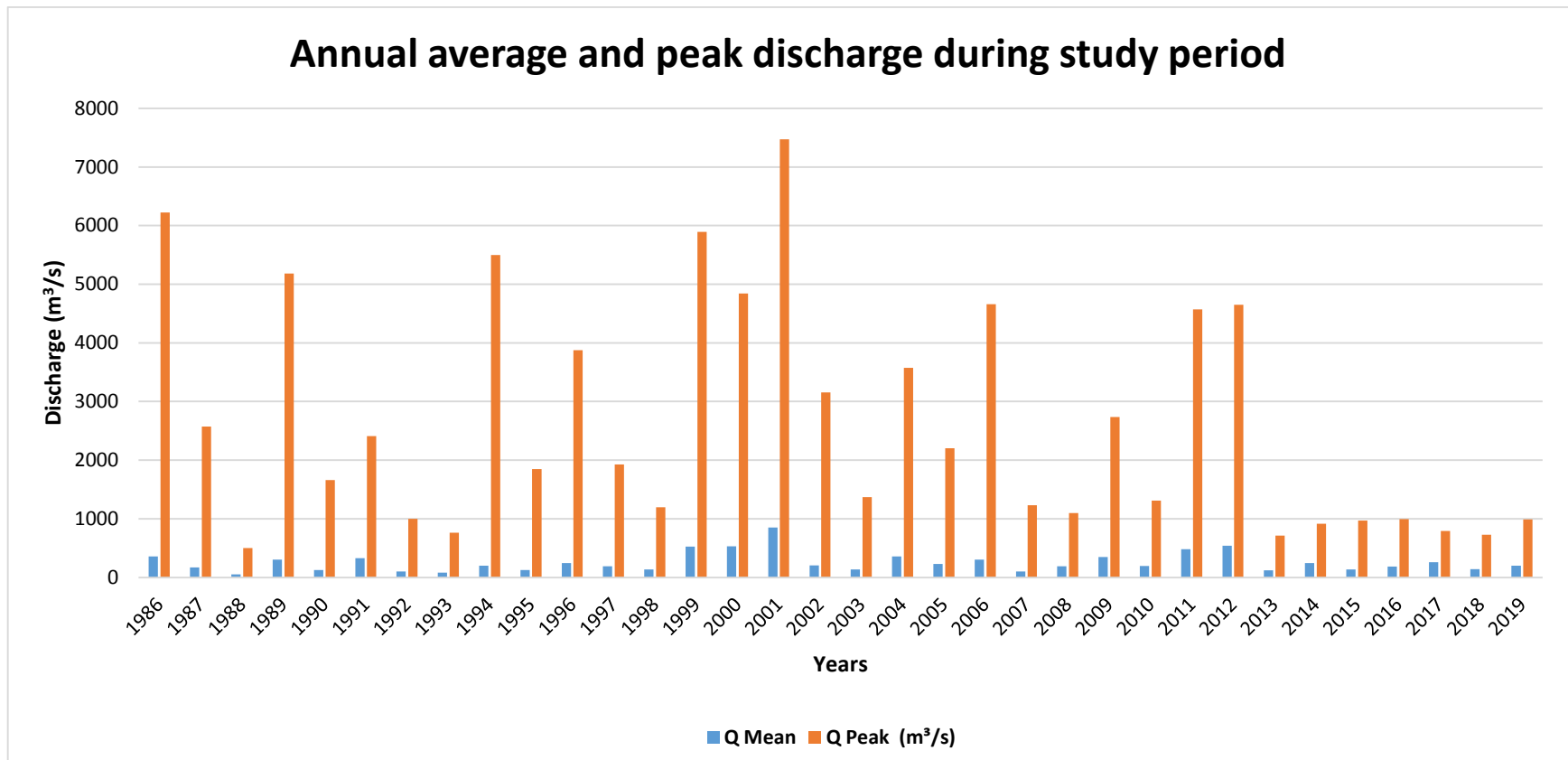


*Figure 6.11 Annual average and peak discharge during study period based on CWC data*

**Table 6.6 Frequency of different recurrence interval discharges in study periods (flood day per year)**

<b>Frequency of different recurrence interval discharges in study periods (flood day per year)</b>						
<b>Years</b>	<b>Q&gt;Q<sub>2</sub></b>	<b>Q&gt;Q<sub>5</sub></b>	<b>Q&gt;Q<sub>10</sub></b>	<b>Q&gt;Q<sub>25</sub></b>	<b>Q&gt;Q<sub>50</sub></b>	<b>Q&gt;Q<sub>100</sub></b>
1990-1994	2.4	0.8	0.2	0	0	0
1995-1999	7.6	3.6	2	0	0	0
2000-2004	17.8	9.2	2.4	0	0	0
2005-2009	5.8	0.4	0	0	0	0
2010-2014	11.4	2.6	0	0	0	0
2015-2019	0	0	0	0	0	0

**Table 6.7 Results of Pearson correlation test between the frequency of hydrological events and geomorphological evolution**

<b>Results of the Pearson correlation test between the frequency of hydrological events and geomorphological evolution</b>						
<b>Years</b>	<b>Q&gt;Q<sub>2</sub></b>	<b>Q&gt;Q<sub>5</sub></b>	<b>Migration</b>	<b>Sinuosity</b>	<b>Width</b>	<b>Radius of Curvature</b>
1990-1994	2.4	0.8	23.22	1.59	208.96	720
1995-1999	7.6	3.6	30.04	1.68	227.13	730
2000-2004	17.8	9.2	35.74	1.82	203.16	760
2005-2009	5.8	0.4	28.25	1.73	243.41	830
2010-2014	11.4	2.6	22.46	1.64	114.01	740
2015-2019	0	0	21.20	1.64	109.95	620

**Table 6.8 Results of Pearson correlation test between the frequency of hydrological events and geomorphological evolution**

<b>Correlation</b>		<b>Migration</b>	<b>Sinuosity</b>	<b>Width</b>	<b>Radius of curvature</b>
<b>Q&gt;Q<sub>2</sub></b>	Pearson correlation	0.76	0.74	0.14	0.78
	Significant	0.07	0.02 *	0.80	0.03 *
<b>Q&gt;Q<sub>5</sub></b>	Pearson correlation	0.89	0.83	0.19	0.65
	Significant	0.04 *	0.08	0.72	0.24 *

\* Significant at 5% confidence level

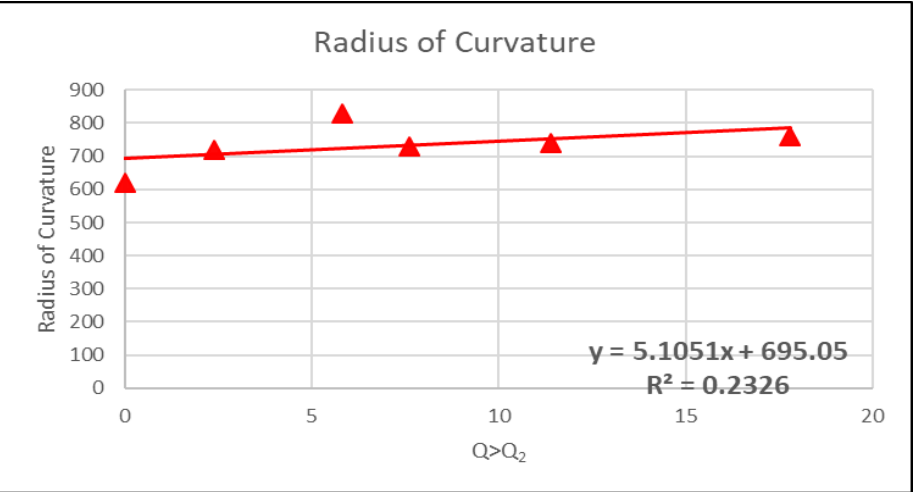
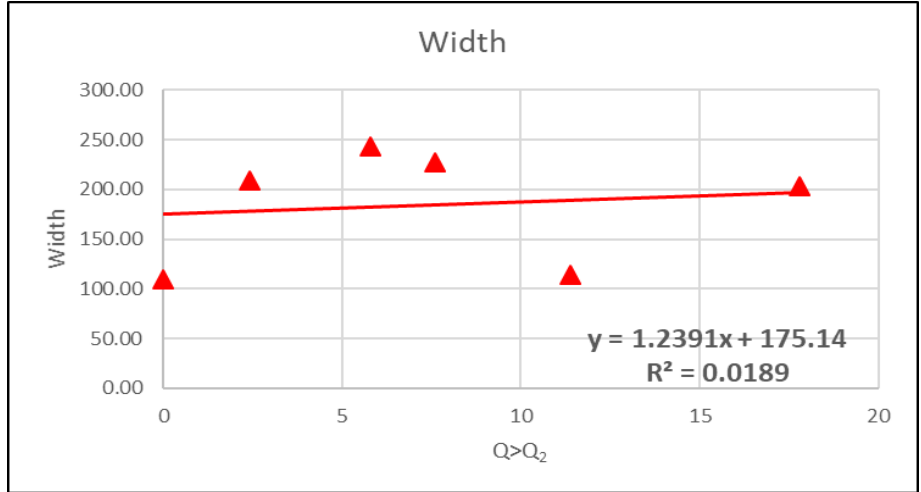
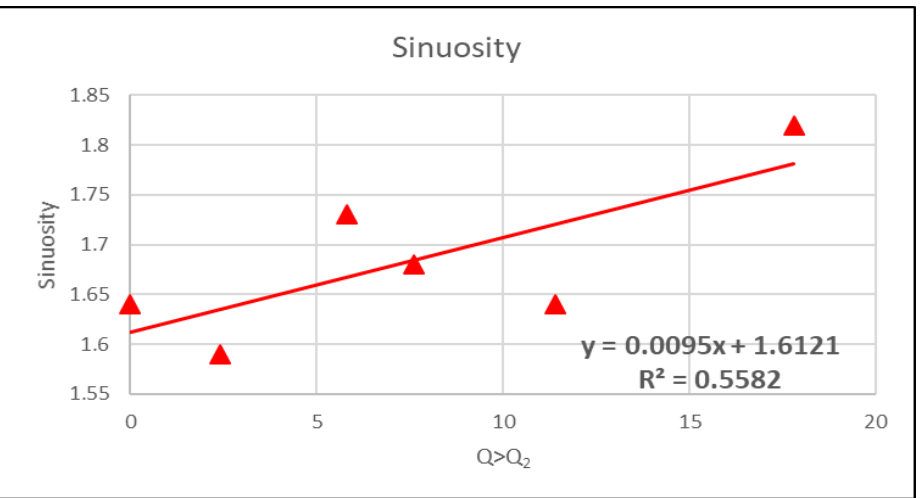
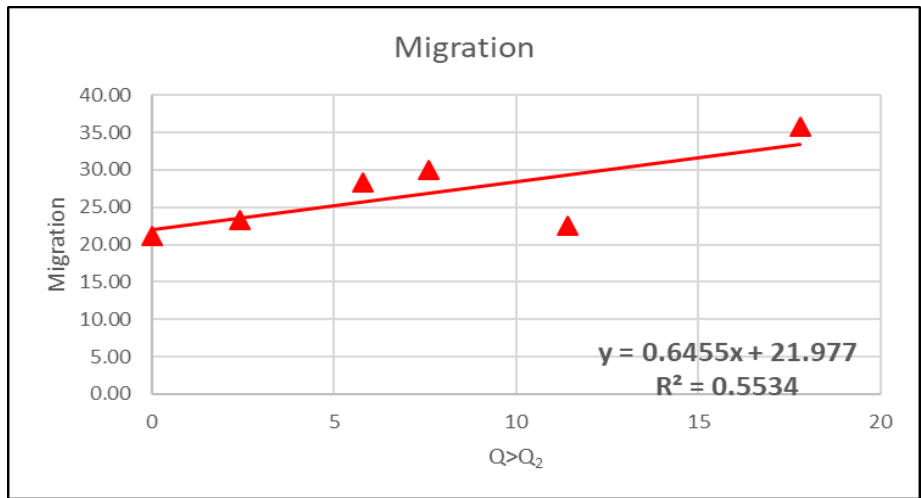


Figure 6.12 Correlation between frequency of hydrological events and geomorphological evolution in the study reach for  $Q > Q_2$

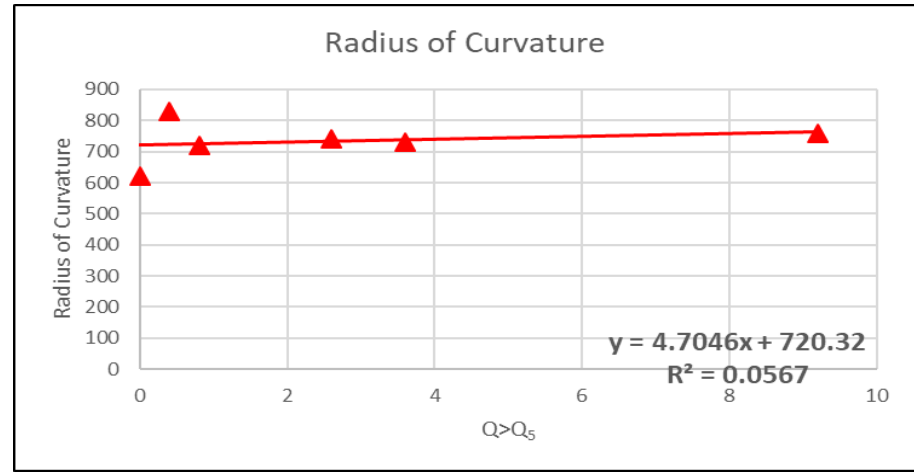
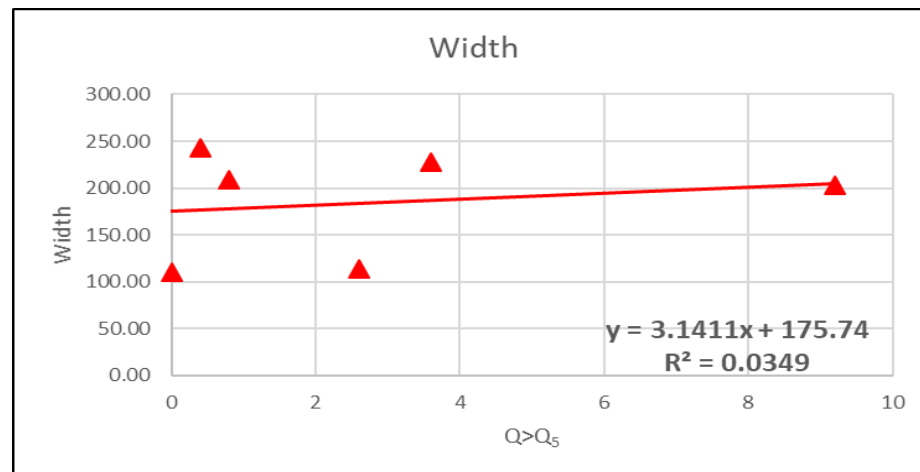
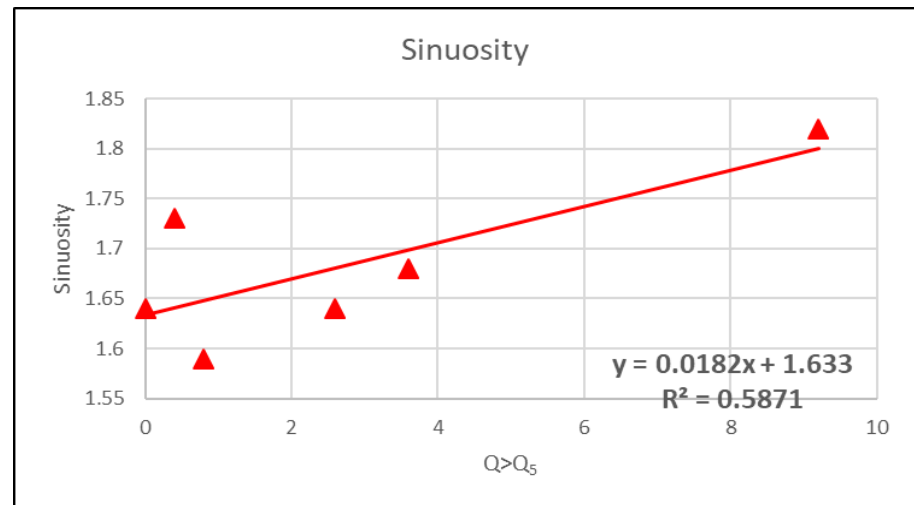
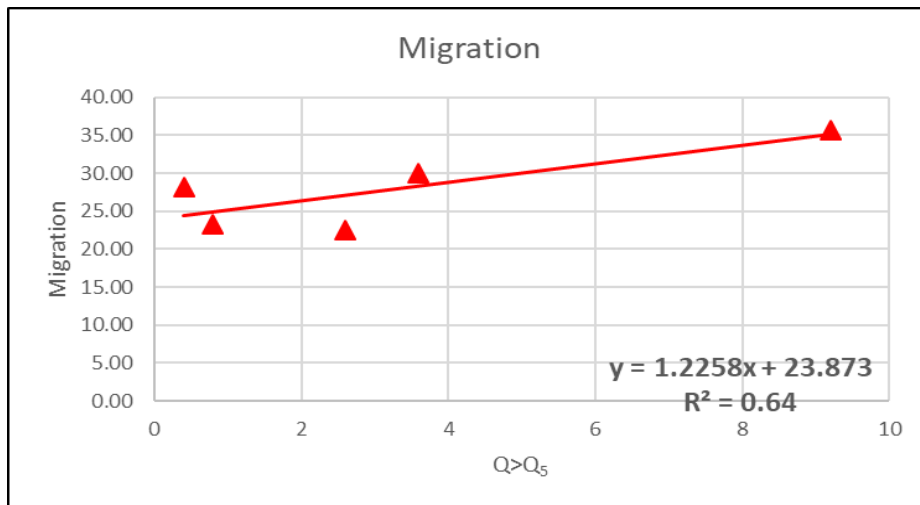


Figure 6.13 Correlation between frequency of hydrological events and geomorphological evolution in the study reach for  $Q > Q_5$

## 6.8 Discussion

### 6.1.7 Geomorphological evolution

Direct and indirect driving forces can change the morphology of fluvial systems. The results of the present study reveal that the study reach of the Ramganga river changed significantly due to flood events. Six new meanders and eleven new cutoffs were formed along the 125 km study reach during 46 years. Once a cutoff has occurred, the flow length decreased, and the sinuosity and curvature will decrease as a consequence [210, 234]. The active channel width reduced significantly by ~43%. No correlation was found between width and floods exceeding  $Q_2$  or  $Q_5$ , suggesting that width change is in response to human activities in the channel [235, 236]. Furthermore, a declining trend in sinuosity index suggests straightening of the channel in the last ~45 year due to cutoff in different meanders. It also gives the impression of direct positive correlation with the lower flood frequency which gives the clues about human intervention in the channel for floodplain management activities. The reduction in the radius of curvature is observed 35% in the 45 years. There is a positive correlation found between the frequency of flood and radius of curvature. It is mainly due to erosion of the channel in the outer side of the meander. The number of cutoffs and new meanders for this period are 4 and 9, respectively, and the movement of the channel is extremely high. Figure 6.9 and 6.10 shows the morphological evolution in some meander loops during the study period. Channel migration was observed highest in the first phase (1973-1981). Another high jump in channel migration is observed during 2000-2010, which is the main cause of channel response to the high discharge (Fig.6.7). The number of new meanders and cutoffs have evolved in this periods are 6 and 11 respectively.

### **6.1.8 Hydrology and Geomorphology**

The availability of hydrological data from 1985 is the main limitation of the study. The Dabri gauging station provides the best option for hydrological analysis in the study area. The results of Pearson correlation test shows that the frequency of hydrological events (flood days) are directly correlated with the sinuosity index and radius of curvature. This indicates that if the number of flood days greater than  $Q_2$  and  $Q_5$  then the length of the channel is expected to increase due to the increase in the sinuous pattern of the river. Hydrological events less than  $Q_5$  play an important role in the formation of meander in the channel by which the channel length will increase [212, 217]. By increasing the frequency of floods bigger than  $Q_5$ , the power of discharge increases, therefore the probability of cutoffs occurring in the channels will be greater. The Channel migration and bank retreat in the study reach have a significant positive correlation with the frequency of floods greater than  $Q_5$ . It is generally accepted that bank retreat occurs during hydrological events larger than average discharge [203, 237, 238]. Depret et al. (2015) stated that increasing the number of flood days directly increased bank retreat and channel migration [235]. Further, the sinuosity index and frequency of hydrological events bigger than  $Q_2$  have a significant positive correlation, but for the frequency of hydrological events bigger than  $Q_5$  has no significant correlation with the sinuosity index. This can be explained with changes in the flow rate of the river. During periods of high discharge, bank retreat and channel movement will straighten the river course via cutoffs [234, 235].

The active channel width of large rivers is mostly controlled by human management activities and very large hydrological events such as flash floods and extreme floods events [217, 241, 242]. Here the results show that the width of the

Ramganga river in the study reach is not significantly correlated with flood frequency (Table 6.6). Some other natural factor also may responsible for average width reduction, e.g. changing river morphology, diversion of river flow, sedimentation process stream flow is the restriction [259]. Therefore, it is likely that channel reinforcement by river managers plays a definitive role in keeping the width of the river stable during larger floods and resulting in an overall narrowing.

## **6.9 Conclusion**

The evolution of the Ramganga river (~ 125 km) has been studied by using available hydrological data during 46 years (1973-2019). The relationship between the frequency of  $Q > Q_2$  and  $Q > Q_5$  and morphological changes in the study reach were considered in particular. Our findings indicate that the study reach of the Ramganga river underwent a significant channel narrowing is due to human intervention (diversion of river flow), rather than any changes in flow magnitude or frequency. The reduction in sinuosity index of the study reach was associated with larger floods causing cutoffs. During this study period, 6 new meanders and 11 cutoffs were formed along the river. Channel migration was higher during a large-flood period in the late 1980s and early 2010s.

Hydrological events with different return periods play important roles in the morphological evolution of the Ramganga river. Cutoffs and higher migration rates are dependent on larger discharge events, while progressive bend development takes place during the periods dominated by smaller flood events. The findings of this study could help to understand the evolution of fluvial systems, mainly where flooding regimes are predictable using hydrological data.